Chapter 18

Cycle expansions

> Recycle... It's the Law!
>
> —Poster, New York City Department of Sanitation

The Euler product representations of spectral determinants (17.9) and dynamical zeta functions (17.15) are really only a shorthand notation - the zeros of the individual factors are *not* the zeros of the zeta function, and convergence of such objects is far from obvious. Now we shall give meaning to the dynamical zeta functions and spectral determinants by expanding them as cycle expansions, series representations ordered by increasing topological cycle length, with products in (17.9), (17.15) expanded as sums over *pseudocycles*, products of t_p's. The zeros of correctly truncated cycle expansions yield the desired eigenvalues, and the expectation values of observables are given by the cycle averaging formulas obtained from the partial derivatives of dynamical zeta functions (or spectral determinants).

18.1 Pseudocycles and shadowing

How are periodic orbit formulas such as (17.15) evaluated? We start by computing the lengths and stability eigenvalues of the shortest cycles. This always requires numerical work, such as the Newton's method searches for periodic solutions; we shall assume that the numerics is under control, and that *all* short cycles up to a given (topological) length have been found. Examples of the data required for application of periodic orbit formulas are the lists of cycles given in tables 26.3 and 12.2. It is important not to miss any short cycles, as the calculation is as accurate as the shortest cycle dropped - including cycles longer than the shortest omitted does not improve the accuracy (more precisely, improves it, but painfully slowly).

Expand the dynamical zeta function (17.15) as a formal power series,

$$1/\zeta = \prod_p (1 - t_p) = 1 - \sum_{\{p_1 p_2 \ldots p_k\}}{}' (-1)^{k+1} t_{p_1} t_{p_2} \ldots t_{p_k} \tag{18.1}$$

where the prime on the sum indicates that the sum is over all distinct non-repeating combinations of prime cycles. As we shall frequently use such sums, let us denote by $t_\pi = (-1)^{k+1} t_{p_1} t_{p_2} \dots t_{p_k}$ an element of the set of all distinct products of the prime cycle weights t_p. The formal power series (18.1) is now compactly written as

$$1/\zeta = 1 - \sum_\pi{}' \, t_\pi \, . \tag{18.2}$$

For $k > 1$, t_π are weights of *pseudocycles*; they are sequences of shorter cycles that shadow a cycle with the symbol sequence $p_1 p_2 \dots p_k$ along segments p_1, $p_2, \dots$, p_k. $\sum'$ denotes the restricted sum, for which any given prime cycle p contributes at most once to a given pseudocycle weight t_π.

The pseudocycle weight, i.e., the product of weights (17.10) of prime cycles comprising the pseudocycle,

$$t_\pi = (-1)^{k+1} \frac{1}{|\Lambda_\pi|} e^{\beta A_\pi - s T_\pi} z^{n_\pi} \, , \tag{18.3}$$

depends on the pseudocycle topological length n_π, integrated observable A_π, period T_π, and stability Λ_π

$$\begin{aligned} n_\pi &= n_{p_1} + \ldots + n_{p_k} \, , \qquad T_\pi = T_{p_1} + \ldots + T_{p_k} \\ A_\pi &= A_{p_1} + \ldots + A_{p_k} \, , \qquad \Lambda_\pi = \Lambda_{p_1} \Lambda_{p_2} \cdots \Lambda_{p_k} \, . \end{aligned} \tag{18.4}$$

Throughout this text, the terms "periodic orbit" and "cycle" are used interchangeably; while "periodic orbit" is more precise, "cycle" (which has many other uses in mathematics) is easier on the ear than "pseudo-periodic-orbit." While in Soviet times acronyms were a rage (and in France they remain so), we shy away from acronyms such as UPOs (Unstable Periodic Orbits).

18.1.1 Curvature expansions

The simplest example is the pseudocycle sum for a system described by a complete binary symbolic dynamics. In this case the Euler product (17.15) is given by

$$\begin{aligned} 1/\zeta &= (1-t_0)(1-t_1)(1-t_{01})(1-t_{001})(1-t_{011}) \\ &\quad (1-t_{0001})(1-t_{0011})(1-t_{0111})(1-t_{00001})(1-t_{00011}) \\ &\quad (1-t_{00101})(1-t_{00111})(1-t_{01011})(1-t_{01111}) \dots \end{aligned} \tag{18.5}$$

(see table 10.1), and the first few terms of the expansion (18.2) ordered by increasing total pseudocycle length are:

$$\begin{aligned} 1/\zeta &= 1 - t_0 - t_1 - t_{01} - t_{001} - t_{011} - t_{0001} - t_{0011} - t_{0111} - \dots \\ &\quad + t_0 t_1 + t_0 t_{01} + t_{01} t_1 + t_0 t_{001} + t_0 t_{011} + t_{001} t_1 + t_{011} t_1 \\ &\quad - t_0 t_{01} t_1 - \dots \end{aligned} \tag{18.6}$$

We refer to such series representation of a dynamical zeta function or a spectral determinant, expanded as a sum over pseudocycles, and ordered by increasing cycle length and instability, as a *cycle expansion*.

The next step is the key step: regroup the terms into the dominant *fundamental* contributions t_f and the decreasing *curvature* corrections $\hat{c}_n$, each $\hat{c}_n$ split into prime cycles p of length $n_p{=}n$ grouped together with pseudocycles whose full itineraries build up the itinerary of p. For the binary case this regrouping is given by

$$\begin{aligned} 1/\zeta &= 1 - t_0 - t_1 - [(t_{01} - t_1 t_0)] - [(t_{001} - t_{01} t_0) + (t_{011} - t_{01} t_1)] \\ &\quad - [(t_{0001} - t_0 t_{001}) + (t_{0111} - t_{011} t_1) \\ &\quad + (t_{0011} - t_{001} t_1 - t_0 t_{011} + t_0 t_{01} t_1)] - \dots \\ &= 1 - \sum_f t_f - \sum_n \hat{c}_n \ . \end{aligned} \tag{18.7}$$

All terms in this expansion up to length $n_p = 6$ are given in table 18.1. We refer to such regrouped series as *curvature expansions*. .

Such separation into "fundamental" and "curvature" parts of cycle expansions is possible *only* for dynamical systems whose symbolic dynamics has finite grammar. The fundamental cycles t_0, t_1 have no shorter approximants; they are the "building blocks" of the dynamics in the sense that all longer orbits can be approximately pieced together from them. The fundamental part of a cycle expansion is given by the sum of the products of all non-intersecting loops of the associated Markov graph. The terms grouped in brackets are the curvature corrections; the terms grouped in parenthesis are combinations of longer cycles and corresponding sequences of "shadowing" pseudocycles. If all orbits are weighted equally ($t_p = z^{n_p}$), such combinations cancel exactly, and the dynamical zeta function reduces to the topological polynomial (13.21). If the flow is continuous and smooth, orbits of similar symbolic dynamics will traverse the same neighborhoods and will have similar weights, and the weights in such combinations will almost cancel. The utility of cycle expansions of dynamical zeta functions and spectral determinants, lies precisely in this organization into nearly canceling combinations: cycle expansions are dominated by short cycles, with long cycles giving exponentially decaying corrections.

☞ sect. 13.3
☞ sect. 18.4

In the case where we know of no finite grammar symbolic dynamics that would help us organize the cycles, the best thing to use is a *stability*

- t_0			
- t_1			
- t_{10}	+ t_1t_0		
- t_{100}	+ $t_{10}t_0$		
- t_{101}	+ $t_{10}t_1$		
- t_{1000}	+ $t_{100}t_0$		
- t_{1001}	+ $t_{100}t_1$	+ $t_{101}t_0$	- $t_1t_{10}t_0$
- t_{1011}	+ $t_{101}t_1$		
- t_{10000}	+ $t_{1000}t_0$		
- t_{10001}	+ $t_{1001}t_0$	+ $t_{1000}t_1$	- $t_0t_{100}t_1$
- t_{10010}	+ $t_{100}t_{10}$		
- t_{10101}	+ $t_{101}t_{10}$		
- t_{10011}	+ $t_{1011}t_0$	+ $t_{1001}t_1$	- $t_0t_{101}t_1$
- t_{10111}	+ $t_{1011}t_1$		
- t_{100000}	+ $t_{10000}t_0$		
- t_{100001}	+ $t_{10001}t_0$	+ $t_{10000}t_1$	- $t_0t_{1000}t_1$
- t_{100010}	+ $t_{10010}t_0$	+ $t_{1000}t_{10}$	- $t_0t_{100}t_{10}$
- t_{100011}	+ $t_{10011}t_0$	+ $t_{10001}t_1$	- $t_0t_{1001}t_1$
- t_{100101}	- t_{100110}	+ $t_{10010}t_1$	+ $t_{10110}t_0$
	+ $t_{10}t_{1001}$	+ $t_{100}t_{101}$	- $t_0t_{10}t_{101}$ - $t_1t_{10}t_{100}$
- t_{101110}	+ $t_{10110}t_1$	+ $t_{1011}t_{10}$	- $t_1t_{101}t_{10}$
- t_{100111}	+ $t_{10011}t_1$	+ $t_{10111}t_0$	- $t_0t_{1011}t_1$
- t_{101111}	+ $t_{10111}t_1$		

Table 18.1: The binary curvature expansion (18.7) up to length 6, listed in such way that the sum of terms along the pth horizontal line is the curvature $\hat{c}_p$ associated with a prime cycle p, or a combination of prime cycles such as the $t_{100101} + t_{100110}$ pair.

cutoff which we shall discuss in sect. 18.5. The idea is to truncate the cycle expansion by including only the pseudocycles such that $|\Lambda_{p_1} \cdots \Lambda_{p_k}| \leq \Lambda_{\max}$, with the cutoff $\Lambda_{\max}$ equal to or greater than the most unstable Λ_p in the data set.

18.2 Construction of cycle expansions

18.2.1 Evaluation of dynamical zeta functions

Cycle expansions of dynamical zeta functions are evaluated numerically by first computing the weights $t_p = t_p(\beta, s)$ of all prime cycles p of topological length $n_p \leq N$ for given fixed β and s. Denote by subscript (i) the ith prime cycle computed, ordered by the topological length $n_{(i)} \leq n_{(i+1)}$. The dynamical zeta function $1/\zeta_N$ truncated to the $n_p \leq N$ cycles is computed recursively, by multiplying

$$1/\zeta_{(i)} = 1/\zeta_{(i-1)}(1 - t_{(i)} z^{n_{(i)}}) \,, \tag{18.8}$$

and truncating the expansion at each step to a finite polynomial in z^n, $n \leq N$. The result is the Nth order polynomial approximation

$$1/\zeta_N = 1 - \sum_{n=1}^{N} c_n z^n \,. \tag{18.9}$$

In other words, a cycle expansion is a Taylor expansion in the dummy variable z raised to the topological cycle length. If both the number of cycles and their individual weights grow not faster than exponentially with the cycle length, and we multiply the weight of each cycle p by a factor z^{n_p}, the cycle expansion converges for sufficiently small $|z|$.

If the dynamics is given by iterated mapping, the leading zero of (18.9) as function of z yields the leading eigenvalue of the appropriate evolution operator. For continuous time flows, z is a dummy variable that we set to $z = 1$, and the leading eigenvalue of the evolution operator is given by the leading zero of (18.9) as function of s.

18.2.2 Evaluation of traces, spectral determinants

Due to the lack of factorization of the full pseudocycle weight,

$$\det\left(\mathbf{1} - M_{p_1 p_2}\right) \neq \det\left(\mathbf{1} - M_{p_1}\right) \det\left(\mathbf{1} - M_{p_2}\right) \,,$$

the cycle expansions for the spectral determinant (17.9) are somewhat less transparent than is the case for the dynamical zeta functions.

We commence the cycle expansion evaluation of a spectral determinant by computing recursively the trace formula (16.10) truncated to all prime cycles p and their repeats such that $n_p r \leq N$:

$$\begin{aligned}
\operatorname{tr} \frac{z\mathcal{L}}{1 - z\mathcal{L}}\Big|_{(i)} &= \operatorname{tr} \frac{z\mathcal{L}}{1 - z\mathcal{L}}\Big|_{(i-1)} + n_{(i)} \sum_{r=1}^{n_{(i)} r \leq N} \frac{e^{(\beta \cdot A_{(i)} - s T_{(i)}) r}}{\left|\prod \left(1 - \Lambda_{(i),j}^{r}\right)\right|} z^{n_{(i)} r} \\
\operatorname{tr} \frac{z\mathcal{L}}{1 - z\mathcal{L}}\Big|_{N} &= \sum_{n=1}^{N} C_n z^n \,, \qquad C_n = \operatorname{tr} \mathcal{L}^n \,.
\end{aligned} \tag{18.10}$$

This is done numerically: the periodic orbit data set consists of the list of the cycle periods T_p, the cycle stability eigenvalues $\Lambda_{p,1}, \Lambda_{p,2}, \ldots, \Lambda_{p,d}$, and the cycle averages of the observable A_p for all prime cycles p such that $n_p \leq N$. The coefficient of $z^{n_p r}$ is then evaluated numerically for the given (β, s) parameter values. Now that we have an expansion for the trace formula (16.9) as a power series, we compute the Nth order approximation to the spectral determinant (17.3),

$$\det\left(1 - z\mathcal{L}\right)\big|_N = 1 - \sum_{n=1}^{N} Q_n z^n \,, \qquad Q_n = n\text{th cumulant} \,, \tag{18.11}$$

as follows. The logarithmic derivative relation (17.4) yields

$$\begin{aligned}\left(\mathrm{tr}\,\frac{z\mathcal{L}}{1-z\mathcal{L}}\right)\det(1-z\mathcal{L}) &= -z\frac{d}{dz}\det(1-z\mathcal{L}) \\ (C_1z+C_2z^2+\cdots)(1-Q_1z-Q_2z^2-\cdots) &= Q_1z+2Q_2z^2+3Q_3z^3\cdots\end{aligned}$$

so the nth order term of the spectral determinant cycle (or in this case, the cumulant) expansion is given recursively by the trace formula expansion coefficients

$$Q_n=\frac{1}{n}\left(C_n-C_{n-1}Q_1-\cdots C_1Q_{n-1}\right)\,,\qquad Q_1=C_1\,. \tag{18.12}$$

Given the trace formula (18.10) truncated to z^N, we now also have the spectral determinant truncated to z^N.

The same program can also be reused to compute the dynamical zeta function cycle expansion (18.9), by replacing $\prod\left(1-\Lambda_{(i),j}^r\right)$ in (18.10) by the product of expanding eigenvalues $\Lambda_{(i)}=\prod_e\Lambda_{(i),e}$ (see sect. 17.3).

The calculation of the leading eigenvalue of a given continuous flow evolution operator is now straightforward. After the prime cycles and the pseudocycles have been grouped into subsets of equal topological length, the dummy variable can be set equal to $z=1$. With $z=1$, expansion (18.11) is the cycle expansion for (17.6), the spectral determinant $\det(s-\mathcal{A})$. We vary s in cycle weights, and determine the eigenvalue s_α by finding $s=s_\alpha$ for which (18.11) vanishes. As an example, the convergence of a leading eigenvalue for a nice hyperbolic system is illustrated in table 18.2 by the listing of pinball escape rate γ estimates computed from truncations of (18.7) and (18.11) to different maximal cycle lengths.

The pleasant surprise is that the coefficients in these cycle expansions can be proven to fall off exponentially or even faster, due to analyticity of $\det(s-\mathcal{A})$ or $1/\zeta(s)$ for s values well beyond those for which the corresponding trace formula diverges.

☞ chapter 20

18.2.3 Newton algorithm for determination of the evolution operator eigenvalues

The cycle expansions of spectral determinants yield the eigenvalues of the evolution operator beyond the leading one. A convenient way to search for these is by plotting either the absolute magnitude $\ln|\det(s-\mathcal{A})|$ or the phase of spectral determinants and dynamical zeta functions as functions of the complex variable s. The eye is guided to the zeros of spectral determinants and dynamical zeta functions by means of complex s plane contour plots, with different intervals of the absolute value of

$R{:}a$	N	. $\det(s-\mathcal{A})$	$1/\zeta(s)$	$1/\zeta(s)_{\text{3-disk}}$
	1	0.39	0.407	
	2	0.4105	0.41028	0.435
	3	0.410338	0.410336	0.4049
6	4	0.4103384074	0.4103383	0.40945
	5	0.4103384077696	0.4103384	0.410367
	6	0.41033840776934648 2	0.4103383	0.410338
	7	0.4103384077693464892		0.4103396
	8	0.41033840776934648933846 8		
	9	0.41033840776934648933846 13074		
	10	0.41033840776934648933846 13078192		
	1	0.41		
	2	0.72		
	3	0.675		
	4	0.67797		
3	5	0.677921		
	6	0.6779227		
	7	0.6779226894		
	8	0.6779226896002		
	9	0.677922689599532		
	10	0.67792268959953606		

Table 18.2: 3-disk repeller escape rates computed from the cycle expansions of the spectral determinant (17.6) and the dynamical zeta function (17.15), as function of the maximal cycle length N. The first column indicates the disk-disk center separation to disk radius ratio $R{:}a$, the second column gives the maximal cycle length used, and the third the estimate of the classical escape rate from the fundamental domain spectral determinant cycle expansion. As for larger disk-disk separations the dynamics is more uniform, the convergence is better for $R{:}a = 6$ than for $R{:}a = 3$. For comparison, the fourth column lists a few estimates from from the fundamental domain dynamical zeta function cycle expansion (18.7), and the fifth from the full 3-disk cycle expansion (18.36). The convergence of the fundamental domain dynamical zeta function is significantly slower than the convergence of the corresponding spectral determinant, and the full (unfactorized) 3-disk dynamical zeta function has still poorer convergence. (P.E. Rosenqvist.)

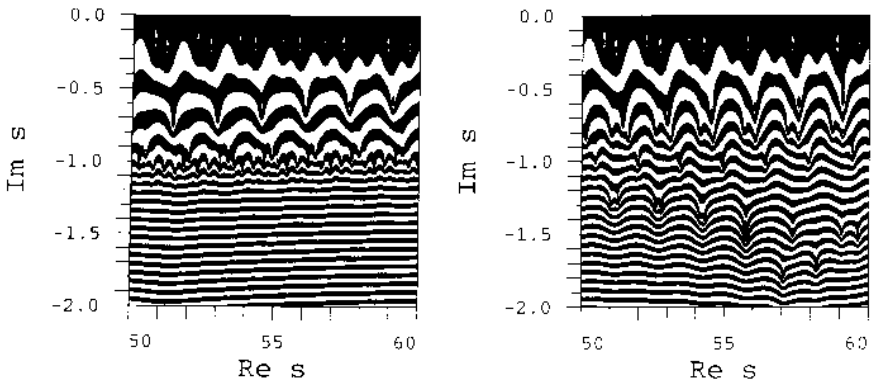

Figure 18.1: Examples of the complex s plane scans: contour plots of the logarithm of the absolute values of (a) $1/\zeta(s)$, (b) spectral determinant $\det(s-\mathcal{A})$ for the 3-disk system, separation $a : R = 6$, A_1 subspace are evaluated numerically. The eigenvalues of the evolution operator $\mathcal{L}$ are given by the centers of elliptic neighborhoods of the rapidly narrowing rings. While the dynamical zeta function is analytic on a strip $\mathrm{Im}\, s \geq -1$, the spectral determinant is entire and reveals further families of zeros. (P.E. Rosenqvist)

the function under investigation assigned different colors; zeros emerge as centers of elliptic neighborhoods of rapidly changing colors. Detailed scans of the whole area of the complex s plane under investigation and searches for the zeros of spectral determinants, figure 18.1, reveal complicated patterns of resonances even for something so simple as the 3-disk game of pinball. With a good starting guess (such as a location of a zero suggested by the complex s scan of figure 18.1), a zero $1/\zeta(s) = 0$ can now be easily determined by standard numerical methods, such as the iterative Newton algorithm (12.4), with the mth Newton estimate given by

$$s_{m+1} = s_m - \left(\zeta(s_m)\frac{\partial}{\partial s}\zeta^{-1}(s_m)\right)^{-1} = s_m - \frac{1/\zeta(s_m)}{\langle T\rangle_\zeta}\ . \tag{18.13}$$

The dominator $\langle T\rangle_\zeta$ required for the Newton iteration is given below, by the cycle expansion (18.22). We need to evaluate it anyhow, as $\langle T\rangle_\zeta$ enters our cycle averaging formulas.

18.3 Cycle formulas for dynamical averages

The eigenvalue condition in any of the three forms that we have given so far - the level sum (19.18), the dynamical zeta function (18.2), the spectral determinant (18.11):

$$1 \;=\; \sum_i^{(n)} t_i\,, \qquad t_i = t_i(\beta, s(\beta))\,, \qquad n_i = n\,, \tag{18.14}$$

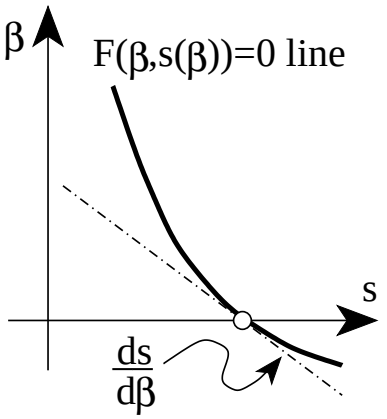

Figure 18.2: The eigenvalue condition is satisfied on the curve $F = 0$ the (β, s) plane. The expectation value of the observable (15.12) is given by the slope of the curve.

$$0 = 1 - \sum_{\pi}{}' t_\pi \,, \qquad t_\pi = t_\pi(z, \beta, s(\beta)) \tag{18.15}$$

$$0 = 1 - \sum_{n=1}^{\infty} Q_n \,, \qquad Q_n = Q_n(\beta, s(\beta)) \,, \tag{18.16}$$

is an implicit equation for the eigenvalue $s = s(\beta)$ of form $F(\beta, s(\beta)) = 0$. The eigenvalue $s = s(\beta)$ as a function of β is sketched in figure 18.2; the eigenvalue condition is satisfied on the curve $F = 0$. The cycle averaging formulas for the slope and the curvature of $s(\beta)$ are obtained as in (15.12) by taking derivatives of the eigenvalue condition. Evaluated along $F = 0$, the first derivative leads to

$$\begin{aligned} 0 &= \frac{d}{d\beta} F(\beta, s(\beta)) \\ &= \frac{\partial F}{\partial \beta} + \frac{ds}{d\beta} \frac{\partial F}{\partial s}\Big|_{s=s(\beta)} \quad \Longrightarrow \quad \frac{ds}{d\beta} = -\frac{\partial F}{\partial \beta} / \frac{\partial F}{\partial s} \,, \end{aligned} \tag{18.17}$$

and the second derivative of $F(\beta, s(\beta)) = 0$ yields

$$\frac{d^2 s}{d\beta^2} = -\left[\frac{\partial^2 F}{\partial \beta^2} + 2 \frac{ds}{d\beta} \frac{\partial^2 F}{\partial \beta \partial s} + \left(\frac{ds}{d\beta} \right)^2 \frac{\partial^2 F}{\partial s^2} \right] / \frac{\partial F}{\partial s} \,. \tag{18.18}$$

Denoting by

$$\begin{aligned} \langle A \rangle_F &= -\frac{\partial F}{\partial \beta}\Big|_{\beta, s=s(\beta)} \,, \qquad \langle T \rangle_F = \frac{\partial F}{\partial s}\Big|_{\beta, s=s(\beta)} \,, \\ \left\langle (A - \langle A \rangle)^2 \right\rangle_F &= \frac{\partial^2 F}{\partial \beta^2}\Big|_{\beta, s=s(\beta)} \end{aligned} \tag{18.19}$$

respectively the mean cycle expectation value of A, the mean cycle period, and the second derivative of F computed for $F(\beta, s(\beta)) = 0$, we obtain the

cycle averaging formulas for the expectation value of the observable (15.12), and its variance:

$$\langle a \rangle = \frac{\langle A \rangle_F}{\langle T \rangle_F} \tag{18.20}$$

$$\left\langle (a - \langle a \rangle)^2 \right\rangle = \frac{1}{\langle T \rangle_F} \left\langle (A - \langle A \rangle)^2 \right\rangle_F . \tag{18.21}$$

These formulas are the central result of the periodic orbit theory. As we shall now show, for each choice of the eigenvalue condition function $F(\beta, s)$ in (19.18), (18.2) and (18.11), the above quantities have explicit cycle expansions.

18.3.1 Dynamical zeta function cycle expansions

For the dynamical zeta function condition (18.15), the cycle averaging formulas (18.17), (18.21) require evaluation of the derivatives of dynamical zeta function at a given eigenvalue. Substituting the cycle expansion (18.2) for dynamical zeta function we obtain

$$\langle A \rangle_\zeta := -\frac{\partial}{\partial \beta} \frac{1}{\zeta} = \sum{}' A_\pi t_\pi \tag{18.22}$$

$$\langle T \rangle_\zeta := \frac{\partial}{\partial s} \frac{1}{\zeta} = \sum{}' T_\pi t_\pi , \quad \langle n \rangle_\zeta := -z \frac{\partial}{\partial z} \frac{1}{\zeta} = \sum{}' n_\pi t_\pi ,$$

where the subscript in $\langle \cdots \rangle_\zeta$ stands for the dynamical zeta function average over prime cycles, A_π, T_π, and n_π are evaluated on pseudocycles (18.4), and pseudocycle weights $t_\pi = t_\pi(z, \beta, s(\beta))$ are evaluated at the eigenvalue $s(\beta)$. In most applications $\beta = 0$, and $s(\beta)$ of interest is typically the leading eigenvalue $s_0 = s_0(0)$ of the evolution generator $\mathcal{A}$.

For bounded flows the leading eigenvalue (the escape rate) vanishes, $s(0) = 0$, the exponent $\beta A_\pi - s T_\pi$ in (18.3) vanishes, so the cycle expansions take a simple form

$$\langle A \rangle_\zeta = \sum_\pi{}' (-1)^{k+1} \frac{A_{p_1} + A_{p_2} \cdots + A_{p_k}}{|\Lambda_{p_1} \cdots \Lambda_{p_k}|} , \tag{18.23}$$

and similarly for $\langle T \rangle_\zeta$, $\langle n \rangle_\zeta$. For example, for the complete binary symbolic dynamics the mean cycle period $\langle T \rangle_\zeta$ is given by

$$\begin{aligned} \langle T \rangle_\zeta = {} & \frac{T_0}{|\Lambda_0|} + \frac{T_1}{|\Lambda_1|} + \left(\frac{T_{01}}{|\Lambda_{01}|} - \frac{T_0 + T_1}{|\Lambda_0 \Lambda_1|} \right) \\ & + \left(\frac{T_{001}}{|\Lambda_{001}|} - \frac{T_{01} + T_0}{|\Lambda_{01} \Lambda_0|} \right) + \left(\frac{T_{011}}{|\Lambda_{011}|} - \frac{T_{01} + T_1}{|\Lambda_{01} \Lambda_1|} \right) + \ldots . \end{aligned} \tag{18.24}$$

Note that the cycle expansions for averages are grouped into the same shadowing combinations as the dynamical zeta function cycle expansion (18.7), with nearby pseudocycles nearly cancelling each other.

The cycle averaging formulas for the expectation value of the observable $\langle a \rangle$ follow by substitution into (18.21). Assuming zero mean drift $\langle a \rangle = 0$, the cycle expansion (18.11) for the variance $\left\langle (A - \langle A \rangle)^2 \right\rangle_\zeta$ is given by

$$\left\langle A^2 \right\rangle_\zeta = \sum{}' (-1)^{k+1} \frac{(A_{p_1} + A_{p_2} \cdots + A_{p_k})^2}{|\Lambda_{p_1} \cdots \Lambda_{p_k}|} \,. \tag{18.25}$$

18.3.2 Spectral determinant cycle expansions

The dynamical zeta function cycle expansions have a particularly simple structure, with the shadowing apparent already by a term-by-term inspection of table 18.2. For "nice" hyperbolic systems the shadowing ensures exponential convergence of the dynamical zeta function cycle expansions. This, however, is not the best achievable convergence. As has been explained in chapter 20, for such systems the spectral determinant constructed from the same cycle data base is entire, and its cycle expansion converges faster than exponentially. In practice, the best convergence is attained by the spectral determinant cycle expansion (18.16) and its derivatives. The $\partial/\partial s$, $\partial/\partial\beta$ derivatives are in this case computed recursively, by taking derivatives of the spectral determinant cycle expansion contributions (18.12) and (18.10).

The cycle averaging formulas are exact, and highly convergent for nice hyperbolic dynamical systems. An example of its utility is the cycle expansion formula for the Lyapunov exponent of example 18.1. Further applications of cycle expansions will be discussed in chapter 19.

18.3.3 Continuous vs. discrete mean return time

Sometimes it is convenient to compute an expectation value along a flow, in continuous time, and sometimes it might be easier to compute it in discrete time, from a Poincaré return map. Return times (3.1) might vary wildly, and it is not at all clear that the continuous and discrete time averages are related in any simple way. The relationship turns on to be both elegantly simple, and totally general.

The mean cycle period $\langle T \rangle_\zeta$ fixes the normalization of the unit of time; it can be interpreted as the average near recurrence or the average first return time. For example, if we have evaluated a billiard expectation value $\langle a \rangle$ in terms of continuous time, and would like to also have the corresponding average $\langle a \rangle_{\rm dscr}$ measured in discrete time, given by the number of reflections off billiard walls, the two averages are related by

$$\langle a \rangle_{\rm dscr} = \langle a \rangle \, \langle T \rangle_\zeta \, / \, \langle n \rangle_\zeta \ , \tag{18.26}$$

where $\langle n \rangle_\zeta$ is the average of the number of bounces n_p along the cycle p.

Example 18.1 Cycle expansion formula for Lyapunov exponents:

In sect. 15.3 we defined the Lyapunov exponent for a 1-d mapping, related it to the leading eigenvalue of an evolution operator and promised to evaluate it. Now we are finally in position to deliver on our promise.

The cycle averaging formula (18.23) yields an exact explict expression for the Lyapunov exponent in terms of prime cycles:

$$\lambda = \frac{1}{\langle n \rangle_\zeta} \sum{}' (-1)^{k+1} \frac{\log|\Lambda_{p_1}| + \cdots + \log|\Lambda_{p_k}|}{|\Lambda_{p_1} \cdots \Lambda_{p_k}|} \ . \tag{18.27}$$

For a repeller, the $1/|\Lambda_p|$ weights are replaced by normalized measure (19.10) $\exp(\gamma n_p)/|\Lambda_p|$, where γ is the escape rate.

We mention here without proof that for 2-d Hamiltonian flows such as our game of pinball there is only one expanding eigenvalue and (18.27) applies as it stands.

in depth:
chapter G.1, p. 755

18.4 Cycle expansions for finite alphabets

A finite Markov graph like the one given in figure 13.3 (d) is a compact encoding of the transition or the Markov matrix for a given subshift. It is a sparse matrix, and the associated determinant (13.17) can be written down by inspection: it is the sum of all possible partitions of the graph into products of non-intersecting loops, with each loop carrying a minus sign:

$$\det(1-T) = 1 - t_0 - t_{0011} - t_{0001} - t_{00011} + t_0 t_{0011} + t_{0011} t_{0001} \tag{18.28}$$

The simplest application of this determinant is to the evaluation of the topological entropy; if we set $t_p = z^{n_p}$, where n_p is the length of the p-cycle, the determinant reduces to the topological polynomial (13.18).

The determinant (18.28) is exact for the finite graph figure 13.3 (e), as well as for the associated finite-dimensional transfer operator of example 15.1. For the associated (infinite dimensional) evolution operator, it is the beginning of the cycle expansion of the corresponding dynamical zeta function:

$$\begin{aligned} 1/\zeta \ &= \ 1 - t_0 - t_{0011} - t_{0001} + t_{0001} t_{0011} \\ &\quad -(t_{00011} - t_0 t_{0011} + \ldots \text{curvatures}) \ldots \end{aligned} \tag{18.29}$$

The cycles $\overline{0}$, $\overline{0001}$ and $\overline{0011}$ are the *fundamental* cycles introduced in (18.7); they are not shadowed by any combinations of shorter cycles, and are the basic building blocks of the dynamics. All other cycles appear together with their shadows (for example, the $t_{00011} - t_0 t_{0011}$ combination) and yield exponentially small corrections for hyperbolic systems.

For the cycle counting purposes both t_{ab} and the pseudocycle combination $t_{a+b} = t_a t_b$ in (18.2) have the same weight $z^{n_a+n_b}$, so all curvature combinations $t_{ab} - t_a t_b$ vanish exactly, and the topological polynomial (13.21) offers a quick way of checking the fundamental part of a cycle expansion.

Since for finite grammars the topological zeta functions reduce to polynomials, we are assured that there are just a few fundamental cycles and that all long cycles can be grouped into curvature combinations. For example, the fundamental cycles in exercise 9.2 are the three 2-cycles which bounce back and forth between two disks and the two 3-cycles which visit every disk. It is only after these fundamental cycles have been included that a cycle expansion is expected to start converging smoothly, i.e., only for n larger than the lengths of the fundamental cycles are the curvatures $\hat{c}_n$ (in expansion (18.7)), a measure of the deviations between long orbits and their short cycle approximants, expected to fall off rapidly with n.

18.5 Stability ordering of cycle expansions

> There is never a second chance. Most often there is not even the first chance.
>
> —John Wilkins

(C.P. Dettmann and P. Cvitanović)

Most dynamical systems of interest have no finite grammar, so at any order in z a cycle expansion may contain unmatched terms which do not fit neatly into the almost cancelling curvature corrections. Similarly, for intermittent systems that we shall discuss in chapter 22, curvature corrections are in general not small, so again the cycle expansions may converge slowly. For such systems schemes which collect the pseudocycle terms according to some criterion other than the topology of the flow may converge more quickly than expansions based on the topological length.

All chaotic systems exhibit some degree of shadowing, and a good truncation criterion should do its best to respect the shadowing at least approximately. If a long cycle is shadowed by two or more shorter cycles and the flow is smooth, the period and the action will be additive in sense that the period of the longer cycle is approximately the sum of the shorter cycle periods. Similarly, stability is multiplicative, so shadowing is approximately preserved by including all terms with pseudocycle stability

$$|\Lambda_{p_1} \cdots \Lambda_{p_k}| \leq \Lambda_{\max} \tag{18.30}$$

and ignoring all more unstable pseudocycles.

Two such schemes for ordering cycle expansions which approximately respect shadowing are truncations by the pseudocycle period (or action) and the stability ordering that we shall discuss here. In these schemes a dynamical zeta function or a spectral determinant is expanded keeping all terms for which the period, action or stability for a combination of cycles (pseudocycle) is less than a given cutoff.

The two settings in which the stability ordering may be preferable to the ordering by topological cycle length are the cases of bad grammar and of intermittency.

18.5.1 Stability ordering for bad grammars

For generic flows it is often not clear what partition of the state space generates the "optimal" symbolic dynamics. Stability ordering does not require understanding dynamics in such detail: if you can find the cycles, you can use stability ordered cycle expansions. Stability truncation is thus easier to implement for a generic dynamical system than the curvature expansions (18.7) which rely on finite subshift approximations to a given flow.

Cycles can be detected numerically by searching a long trajectory for near recurrences. The long trajectory method for detecting cycles preferentially finds the least unstable cycles, regardless of their topological length. Another practical advantage of the method (in contrast to Newton method searches) is that it only finds cycles in a given connected ergodic component of state space, ignoring isolated cycles or other ergodic regions elsewhere in the state space.

Why should stability ordered cycle expansion of a dynamical zeta function converge better than the rude trace formula (19.9)? The argument has essentially already been laid out in sect. 13.7: in truncations that respect shadowing most of the pseudocycles appear in shadowing combinations and nearly cancel, while only the relatively small subset affected by the longer and longer pruning rules is not shadowed. So the error is typically of the order of $1/\Lambda$, smaller by factor e^{hT} than the trace formula (19.9) error, where h is the entropy and T typical cycle length for cycles of stability Λ.

18.5.2 Smoothing

The breaking of exact shadowing cancellations deserves further comment. Partial shadowing which may be present can be (partially) restored by smoothing the stability ordered cycle expansions by replacing the $1/\Lambda$ weight for each term with pseudocycle stability $\Lambda = \Lambda_{p_1} \cdots \Lambda_{p_k}$ by

$f(\Lambda)/\Lambda$. Here, $f(\Lambda)$ is a monotonically decreasing function from $f(0) = 1$ to $f(\Lambda_{\max}) = 0$. No smoothing corresponds to a step function.

A typical "shadowing error" induced by the cutoff is due to two pseudocycles of stability Λ separated by $\Delta\Lambda$, and whose contribution is of opposite signs. Ignoring possible weighting factors the magnitude of the resulting term is of order $1/\Lambda - 1/(\Lambda + \Delta\Lambda) \approx \Delta\Lambda/\Lambda^2$. With smoothing there is an extra term of the form $f'(\Lambda)\Delta\Lambda/\Lambda$, which we want to minimise. A reasonable guess might be to keep $f'(\Lambda)/\Lambda$ constant and as small as possible, that is

$$f(\Lambda) = 1 - \left(\frac{\Lambda}{\Lambda_{\max}}\right)^2$$

The results of a stability ordered expansion (18.30) should always be tested for robustness by varying the cutoff $\Lambda_{\max}$. If this introduces significant variations, smoothing is probably necessary.

18.5.3 Stability ordering for intermittent flows

Longer but less unstable cycles can give larger contributions to a cycle expansion than short but highly unstable cycles. In such situation truncation by length may require an exponentially large number of very unstable cycles before a significant longer cycle is first included in the expansion. This situation is best illustrated by intermittent maps that we shall study in detail in chapter 22, the simplest of which is the Farey map

$$f(x) = \begin{cases} f_0 = x/(1-x) & 0 \le x \le 1/2 \\ f_1 = (1-x)/x & 1/2 \le x \le 1 \end{cases} , \tag{18.31}$$

a map which will reappear in the intermittency chapter 22, and in chapter 27, in context of circle maps.

For this map the symbolic dynamics is of complete binary type, so lack of shadowing is not due to lack of a finite grammar, but rather to the intermittency caused by the existence of the marginal fixed point $x_0 = 0$, for which the stability equals $\Lambda_0 = 1$. This fixed point does not participate directly in the dynamics and is omitted from cycle expansions. Its presence is felt in the stabilities of neighboring cycles with n consecutive repeats of the symbol 0's whose stability falls of only as $\Lambda \sim n^2$, in contrast to the most unstable cycles with n consecutive 1's which are exponentially unstable, $|\Lambda_{01^n}| \sim [(\sqrt{5}+1)/2]^{2n}$.

The symbolic dynamics is of complete binary type. A quick count in the style of sect. 13.5.2 leads to a total of 74,248,450 prime cycles of length 30 or less, not including the marginal point $x_0 = 0$. Evaluating a cycle expansion

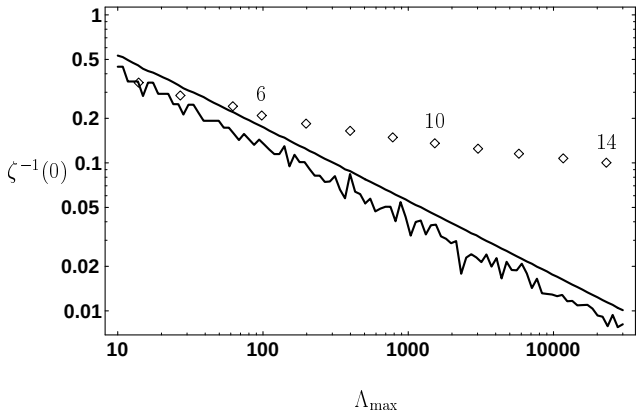

Figure 18.3: Comparison of cycle expansion truncation schemes for the Farey map (18.31); the deviation of the truncated cycles expansion for $|1/\zeta_N(0)|$ from the exact flow conservation value $1/\zeta(0) = 0$ is a measure of the accuracy of the truncation. The jagged line is logarithm of the stability ordering truncation error; the smooth line is smoothed according to sect. 18.5.2; the diamonds indicate the error due the topological length truncation, with the maximal cycle length N shown. They are placed along the stability cutoff axis at points determined by the condition that the total number of cycles is the same for both truncation schemes.

to this order would be no mean computational feat. However, the least unstable cycle omitted has stability of roughly $\Lambda_{10^{30}} \sim 30^2 = 900$, and so amounts to a 0.1% correction. The situation may be much worse than this estimate suggests, because the next, 10^{31} cycle contributes a similar amount, and could easily reinforce the error. Adding up all such omitted terms, we arrive at an estimated error of about 3%, for a cycle-length truncated cycle expansion based on more than 10^9 pseudocycle terms! On the other hand, truncating by stability at say $\Lambda_{\max} = 3000$, only 409 prime cycles suffice to attain the same accuracy of about 3% error, figure 18.3.

As the Farey map maps the unit interval onto itself, the leading eigenvalue of the Perron-Frobenius operator should equal $s_0 = 0$, so $1/\zeta(0) = 0$. Deviation from this exact result serves as an indication of the convergence of a given cycle expansion. The errors of different truncation schemes are indicated in figure 18.3. We see that topological length truncation schemes are hopelessly bad in this case; stability length truncations are somewhat better, but still rather bad. In simple cases like this one, where intermittency is caused by a single marginal fixed point, the convergence can be improved by going to infinite alphabets.

18.6 Dirichlet series

> The most patient reader will thank me for compressing so much nonsense and falsehood into a few lines.
>
> —Gibbon

A Dirichlet series is defined as

$$f(s) = \sum_{j=1}^{\infty} a_j e^{-\lambda_j s} \tag{18.32}$$

where s, a_j are complex numbers, and $\{\lambda_j\}$ is a monotonically increasing series of real numbers $\lambda_1 < \lambda_2 < \cdots < \lambda_j < \cdots$. A classical example of a Dirichlet series is the Riemann zeta function for which $a_j = 1$, $\lambda_j = \ln j$. In the present context, formal series over individual pseudocycles such as (18.2) ordered by the increasing pseudocycle periods are often Dirichlet series. For example, for the pseudocycle weight (18.3), the Dirichlet series is obtained by ordering pseudocycles by increasing periods $\lambda_\pi = T_{p_1} + T_{p_2} + \ldots + T_{p_k}$, with the coefficients

$$a_\pi = \frac{e^{\beta\cdot(A_{p_1}+A_{p_2}+\ldots+A_{p_k})}}{|\Lambda_{p_1}\Lambda_{p_2}\ldots\Lambda_{p_k}|} d_\pi \,,$$

where d_π is a degeneracy factor, in the case that d_π pseudocycles have the same weight.

If the series $\sum |a_j|$ diverges, the Dirichlet series is absolutely convergent for $\mathrm{Re}\, s > \sigma_{\rm a}$ and conditionally convergent for $\mathrm{Re}\, s > \sigma_{\rm c}$, where σ_a is the *abscissa of absolute convergence*

$$\sigma_a = \lim_{N\to\infty} \sup \frac{1}{\lambda_N} \ln \sum_{j=1}^{N} |a_j| \,, \tag{18.33}$$

and σ_c is the *abscissa of conditional convergence*

$$\sigma_c = \lim_{N\to\infty} \sup \frac{1}{\lambda_N} \ln \left| \sum_{j=1}^{N} a_j \right| \,. \tag{18.34}$$

We shall encounter another example of a Dirichlet series in the semiclassical quantization chapter 31, where the inverse Planck constant is a complex variable $s = i/\hbar$, $\lambda_\pi = S_{p_1} + S_{p_2} + \ldots + S_{p_k}$ is the pseudocycle action, and $a_\pi = 1/\sqrt{|\Lambda_{p_1}\Lambda_{p_2}\ldots\Lambda_{p_k}|}$ (times possible degeneracy and topological phase factors). As the action is in general not a linear function of energy (except for billiards and for scaling potentials, where a variable s can be extracted from S_p), semiclassical cycle expansions are Dirichlet series in variable $s = i/\hbar$ but not in E, the complex energy variable.

Résumé

A *cycle expansion* is a series representation of a dynamical zeta function, trace formula or a spectral determinant, with products in (17.15), (32.18) expanded as sums over *pseudocycles*, products of the prime cycle weights t_p.

If a flow is hyperbolic and has a topology of a Smale horseshoe (a subshift of finite type), the dynamical zeta functions are holomorphic, the spectral determinants are entire, and the spectrum of the evolution operator is discrete. The situation is considerably more reassuring than what practitioners of quantum chaos fear; there is no "abscissa of absolute convergence" and no "entropy barier", the exponential proliferation of cycles is no problem, spectral determinants are entire and converge everywhere, and the topology dictates the choice of cycles to be used in cycle expansion truncations.

In that case, the basic observation is that the motion in dynamical systems of few degrees of freedom is in this case organized around a few *fundamental* cycles, with the cycle expansion of the Euler product

$$1/\zeta = 1 - \sum_f t_f - \sum_n \hat{c}_n,$$

regrouped into dominant *fundamental* contributions t_f and decreasing *curvature* corrections $\hat{c}_n$. The fundamental cycles t_f have no shorter approximants; they are the "building blocks" of the dynamics in the sense that all longer orbits can be approximately pieced together from them. A typical curvature contribution to $\hat{c}_n$ is a *difference* of a long cycle $\{ab\}$ minus its shadowing approximation by shorter cycles $\{a\}$ and $\{b\}$:

$$t_{ab} - t_a t_b = t_{ab}(1 - t_a t_b/t_{ab})$$

The orbits that follow the same symbolic dynamics, such as $\{ab\}$ and a "pseudocycle" $\{a\}\{b\}$, lie close to each other, have similar weights, and for longer and longer orbits the curvature corrections fall off rapidly. Indeed, for systems that satisfy the "axiom A" requirements, such as the 3-disk billiard, curvature expansions converge very well.

Once a set of the shortest cycles has been found, and the cycle periods, stabilities and integrated observable computed, the cycle averaging formulas such as the ones associated with the dynamical zeta function

$$\begin{aligned} \langle a \rangle &= \langle A \rangle_\zeta \,/\, \langle T \rangle_\zeta \\ \langle A \rangle_\zeta &= -\frac{\partial}{\partial \beta}\frac{1}{\zeta} = {\sum}' A_\pi t_\pi \,, \qquad \langle T \rangle_\zeta = \frac{\partial}{\partial s}\frac{1}{\zeta} = {\sum}' T_\pi t_\pi \end{aligned}$$

yield the expectation value (the chaotic, ergodic average over the non–wandering set) of the observable $a(x)$.

Commentary

Remark 18.1 Pseudocycle expansions. Bowen's introduction of shadowing ϵ-pseudoorbits [1.23] was a significant contribution to Smale's theory. Expression "pseudoorbits" seems to have been introduced in the Parry and Pollicott's 1983 paper [17.5]. Following them M. Berry [18.9] had used the expression "pseudoorbits" in his 1986 paper on Riemann zeta and quantum chaos. Cycle and curvature expansions of dynamical zeta functions and spectral determinants were introduced in refs. [18.10, 18.2]. Some literature [17.14] refers to the pseudoorbits as "composite orbits", and to the cycle expansions as "Dirichlet series" (see also remark 18.6 and sect. 18.6).

Remark 18.2 Cumulant expansion. To a statistical mechanician the curvature expansions are very reminiscent of cumulant expansions. Indeed, (18.12) is the standard Plemelj-Smithies cumulant formula (J.28) for the Fredholm determinant, discussed in more detail in appendix J. The difference is that in cycle expansions each Q_n coefficient is expressed as a sum over exponentially many cycles.

Remark 18.3 Exponential growth of the number of cycles. Going from $N_n \approx N^n$ periodic points of length n to M_n prime cycles reduces the number of computations from N_n to $M_n \approx N^{n-1}/n$. Use of discrete symmetries (chapter **??**) reduces the number of nth level terms by another factor. While the reformulation of the theory from the trace (16.28) to the cycle expansion (18.7) thus does not eliminate the exponential growth in the number of cycles, in practice only the shortest cycles are used, and for them the computational labor saving can be significant.

Remark 18.4 Shadowing cycle-by-cycle. A glance at the low order curvatures in the table 18.1 leads to the temptation of associating curvatures to individual cycles, such as $\hat{c}_{0001} = t_{0001} - t_0 t_{001}$. Such combinations tend to be numerically small (see for example ref. [18.3], table 1). However, splitting $\hat{c}_n$ into individual cycle curvatures is not possible in general [10.20]; the first example of such ambiguity in the binary cycle expansion is given by the t_{100101}, t_{100110} $0 \leftrightarrow 1$ symmetric pair of 6-cycles; the counterterm $t_{001}t_{011}$ in table 18.1 is shared by the two cycles.

Remark 18.5 Stability ordering. The stability ordering was introduced by Dahlqvist and Russberg [18.12] in a study of chaotic dynamics for the $(x^2y^2)^{1/a}$ potential. The presentation here runs along the lines of Dettmann and Morriss [18.13] for the Lorentz gas which is hyperbolic but the symbolic dynamics is highly pruned, and Dettmann and Cvitanović [18.14] for a family of intermittent maps. In the applications discussed in the above papers, the stability ordering yields a considerable improvement over the topological length ordering. In quantum chaos applications cycle expansion cancelations are affected by the phases of pseudocycles (their actions), hence *period ordering* rather than stability is frequently employed.

Remark 18.6 Are cycle expansions Dirichlet series?

Even though some literature [17.14] refers to cycle expansions as "Dirichlet series", they are not Dirichlet series. Cycle expansions collect contributions of individual cycles into groups that correspond to the coefficients in cumulant expansions of spectral determinants, and the convergence of cycle expansions is controlled by general properties of spectral determinants. Dirichlet series order cycles by their periods or actions, and are only conditionally convergent in regions of interest. The abscissa of absolute convergence is in this context called the "entropy barrier"; contrary to the frequently voiced anxieties, this number does not necessarily has much to do with the actual convergence of the theory.

References

[18.1] P. Cvitanović, *Phys. Rev. Lett.* **61**, 2729 (1988).

[18.2] R. Artuso, E. Aurell and P. Cvitanović, "Recycling of strange sets I: Cycle expansions", *Nonlinearity* **3**, 325 (1990).

[18.3] R. Artuso, E. Aurell and P. Cvitanović, "Recycling of strange sets II: Applications", *Nonlinearity* **3**, 361 (1990).

[18.4] S. Grossmann and S. Thomae, *Z. Naturforsch.* **32 a**, 1353 (1977); reprinted in ref. [18.5].

[18.5] *Universality in Chaos*, P. Cvitanović, ed., (Adam Hilger, Bristol 1989).

[18.6] F. Christiansen, P. Cvitanović and H.H. Rugh, *J. Phys* **A 23**, L713 (1990).

[18.7] J. Plemelj, *"Zur Theorie der Fredholmschen Funktionalgleichung"*, *Monat. Math. Phys.* **15**, 93 (1909).

[18.8] F. Smithies, *"The Fredholm theory of integral equations"*, *Duke Math.* **8**, 107 (1941).

[18.9] M.V. Berry, in *Quantum Chaos and Statistical Nuclear Physics*, ed. T.H. Seligman and H. Nishioka, *Lecture Notes in Physics* **263**, 1 (Springer, Berlin, 1986).

[18.10] P. Cvitanović, *"Invariant measurements of strange sets in terms of cycles"*, *Phys. Rev. Lett.* **61**, 2729 (1988).

[18.11] B. Eckhardt and G. Russberg, *Phys. Rev.* **E 47**, 1578 (1993).

[18.12] P. Dahlqvist and G. Russberg, *"Periodic orbit quantization of bound chaotic systems"*, *J. Phys.* **A 24**, 4763 (1991); P. Dahlqvist *J. Phys.* **A 27**, 763 (1994).

[18.13] C. P. Dettmann and G. P. Morriss, *Phys. Rev. Lett.* **78**, 4201 (1997).

[18.14] C. P. Dettmann and P. Cvitanović, *Cycle expansions for intermittent diffusion Phys. Rev. E* **56**, 6687 (1997); chao-dyn/9708011.